applied sciences

MDPI

Article

Effects of Aggregate Micro Fines (AMF), Aluminum Sulfate and Polypropylene Fiber (PPF) on Properties of Machine-Made Sand Concrete

Hang He [1], Yuli Wang [1] and Junjie Wang [2,*]

[1] School of Materials Science and Engineering, Henan Polytechnic University, Jiaozuo 454003, China; 211606020018@home.hpu.edu.cn (H.H.); wangyuli@hpu.edu.cn (Y.W.)

[2] Division of Engineering, New York University Abu Dhabi, Abu Dhabi, P.O. Box 129188, UAE

* Correspondence: jw4777@nyu.edu; Tel.: +97-126-284-930

Received: 5 May 2019; Accepted: 24 May 2019; Published: 31 May 2019

Featured Application: The research could contribute to the understanding of the mix design of machine-made sand concrete with aggregate micro fines (AMF), aluminum sulfate, and polypropylene fiber.

Abstract: With the depletion and increasing demand of river sand, machine-made sand could be used more and more in concrete. In order to improve the properties of machine-made sand concrete, the effects of the aggregate micro fines (AMF) content, aluminum sulfate, and polypropylene fibers (PPF) on the slump, compressive strength, water permeability, and the chloride permeability coefficients were investigated through a single factor test method, and related mechanisms were analyzed. The results show that the optimum contents of AMF, aluminum sulfate, and the polypropylene fiber are 10 wt%, 1 wt%, and 0.6 kg/m^3, respectively. The optimum content of AMF improved the compactness of concrete. The addition of aluminum sulfate promoted the initial formation of ettringite, and thereby improved the compressive strength and the permeability resistance. The polypropylene fiber can modify the pore structure distribution of concrete and reduce the porosity, thereby improving the impermeability of the concrete. The compressive strength of the machine-made sand concrete could be increased by more than 20%, and the water/chloride permeability coefficients could be decreased by more than 45%.

Keywords: aggregate micro fines; machine-made sand; concrete; aluminum sulfate; polypropylene fiber; performance

1. Introduction

With the rapid development of China, the massive projects in civil engineering require more and more river sand as normal fine aggregates based on the main trend in concrete design. The depletion of river sand could happen in a number of places, especially places that are further away from any rivers. In this condition, the use of machine-made sand [1–3] could be an easy and feasible option. Compared to river sand, machine-made sand has several advantages, such as the existence of aggregate micro fines (AMF). There have been conflicting reports on the role of AMF [4–7] on the properties of machine-made sand concrete (MSC). Some researchers [8–10] reported a decreased slump and an increase in water demand in the MSC with an increase in AMF content. Others [11–14] reported that there is an optimum content of AMF for the properties of MSC, and the existence of AMF could contribute to a higher compressive strength. For example, Shen et al. [11] reported that the highest compressive strength of MSC was achieved when there was 7.5% AMF in the machine-made sand. However, the compressive strength was reported to be influenced by many different factors [15], and this could result in the different reported findings. It can be concluded that the effect of AMF on the concrete properties requires further investigations, especially in MSC. It was found that the effect of AMF on the theology of cement paste was influenced by the surface property, particle size, and also the mineral types [16]. Wang et al. [14] provided a theory analysis based on the physical and mathematical packing model.

In order to modify the properties of concrete, the polypropylene fiber (PPF) could be added [17–28], and the PPF was found to be very effective in improving the crack resistance compared to other methods. The addition of PPF was found to decrease the workability [17] and increase the compressive strength [29–32], crack resistance [33–35], and durability [31,36–41] given that the PPF was within an optimum content. The addition of fibers in concrete can also decrease the shrinkage and reduce the porosity [42,43]. However, the addition of PPF in MSC has rarely been reported, and the optimum content of PPF in MSC is still unknown.

In addition, the use of aluminum sulfate in the concrete could be beneficial because the aluminum sulfate could react with CaO or $Ca(OH)_2$ to form the ettringite and thereby decrease the permeability and increase the compaction of concrete [44–46], but the use of aluminum sulfate in MSC has not been investigated before.

Therefore, in this study, the optimum content of AMF and its effect on the properties of MSC (including slump, compressive strength, and permeability) were investigated. In addition, based on the optimum content of AMF, the effects of aluminum sulfate and polypropylene fiber on the properties of MSC were studied, and the related mechanisms were analyzed.

2. Materials and Methods

2.1. Materials

Ordinary Portland cement (OPC) (Solid Cement Co., Ltd., Jiaozuo, China) with a Grade of 42.5 confirming to GB 175-2007 [47] was used. The coarse aggregate used was a continuous graded gravel of 5 to 25 mm with an apparent density of 2721 kg/m^3, bulk density of 1562 kg/m^3, void ratio of 42.6%, and a crushing value of 7.5%. The main properties of machine-made sand (MS) are shown in Table 1. The AMF (Qiangnai Co., Ltd., Jiaozuo, China) was added into machine-made sand by equal mass to adjust the content of AMF. The particle size distributions of the gravel, MS, and AMF are shown in Figure 1. The XRD result of AMF is shown in Figure 1d, and the main component is $CaCO_3$. The chemical reagent aluminum sulfate (Luoyang Chemical Reagent Factory, Luoyang, China) was used, and its chemical formula is $Al_2(SO_4)_3{\cdot}18H_2O$, and the effective dosage is 99 wt%. The PPF (Lixing Chemical, Zhengzhou, China) used had a modulus of elasticity at 3.8 GPa and a length/diameter ratio of 60. Polycarboxylate superplasticizer was used. Local tap water was used for concrete casting.

Table 1. Properties of machine-made sand.

Density (×10^3 kg/m^3)			Air Void Ratio (%)	Fineness Modulus	AMF [1] Content (%)	MB [2]	Crushing Index (%)	Roughness (%)
Apparent	Bulk	Tight						
2.69	1.55	1.82	42.0	3.10	4.3	0.5	18	18.9

[1] AMF—aggregate micro fines. [2] MB—methylene blue value.

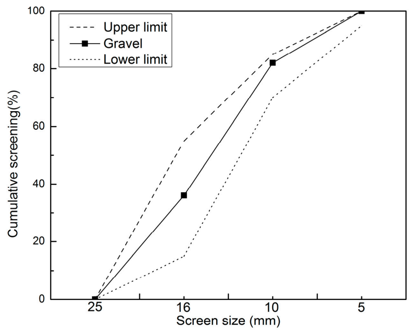

(**a**)

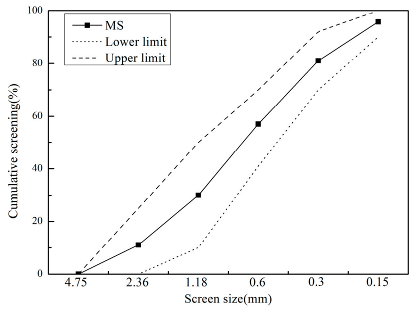

(**b**)

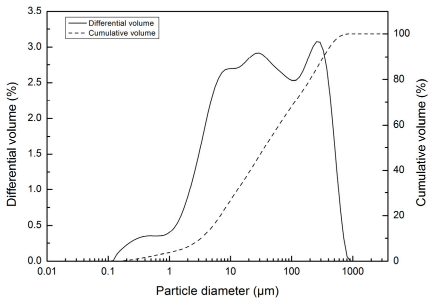

(**c**)

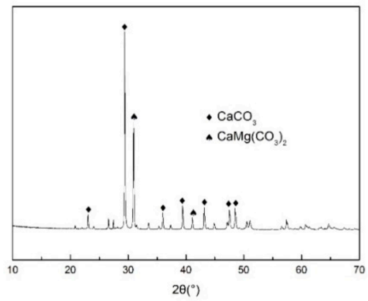

(**d**)

Figure 1. Particle size distribution and XRD: (**a**) particle size distribution of gravel conforming to [48]; (**b**) particle size distribution of machine-made sand (MS) conforming to [49]; (**c**) particle size distribution of aggregate micro fines (AMF), and (**d**) XRD result of AMF.

2.2. Mix Design

The mix design is shown in Table 2. Firstly, the AMF content considered was 0%, 5%, 10%, 15%, and 20% by weight of machine-made sand. Secondly, based on the 10% AMF (optimum content based on initial trails), the addition of aluminum sulfate was based on the weight percentage of cementitious materials (OPC and superplasticizer) by 0%, 0.5%, 1.0% and 2.0%. Lastly, based on the 10% AMF and 1% aluminum sulfate (optimum content), the content of PPF considered was 0, 0.6, 0.9, and 1.35 kg/m^3. Fresh concrete was cast into different molds and covered with a plastic sheet to prevent any water evaporation. The specimens were demolded after 24 h and cured under a standard environment (95% RH and 20 ± 2 °C).

Table 2. Mix design.

Groups	AS [1] (wt%)	PPF [2] (kg/m^3)	AMF Content (wt%)	Raw Material (kg/m^3)				
				OPC	Gravel	MS [3]	Water	Superplasticizer
NO.1			0					
NO.2			5					
NO.3	—	—	10					
NO.4			15					
NO.5			20					
NO.6	0.5			380	1120	750	190	2.28
NO.7	1.0	—	10					
NO.8	2.0							
NO.9		0.6						
NO.10	1.0	0.9	10					
NO.11		1.35						

[1] AS—aluminum sulfate. [2] PPF—polypropylene fiber. [3] MS—machine-made sand.

2.3. Test Methods

2.3.1. Slump and Compressive Strength Tests

Concrete slump and compressive strength were tested in accordance with the Chinese National Standard GB/T 50080-2016 [50]. The test piece size of the concrete compressive strength was 150 mm × 150 mm × 150 mm. The loading speed was 0.5–0.8 MPa/s. The average result of 3 replicate specimens were obtained for each mix group.

2.3.2. Chloride Permeability Test

The chloride permeability coefficient of concrete was measured by the Nernst–Einstein–Lu (NEL) method [51,52] based on the Nernst–Einstein equation. After 28 days, a 100 mm × 100 mm × 400 mm concrete specimen was cut into three samples with a size of 100 mm × 100 mm × 50 mm, and the two test faces which needed to be in contact with the electrodes were polished. The sample was placed in a 4.0 mol/L NaCl solution under vacuum condition (2 kPa) for 24 h in order to achieve a salt-saturated state, and then it was tested by an NEL-PD type concrete chloride permeability test system under a low voltage at around 5 V. The concrete sample was in contact with the two electrodes in the test chamber under the test. The chloride permeability coefficient in concrete is calculated by Equation (1):

$$D_{cl} = f\frac{RT\sigma}{F^2 C_{cl}} \tag{1}$$

where D_{cl} is the chloride permeability coefficient, m^2/s; R is the gas constant, 8.314 J/mol·k; T is the absolute temperature, K; σ is the electrical conductivity of salt-saturated concrete, S/m; F is the Faraday constant, 96,500 C/mol; C_{cl} is the concentration of chloride ion in the pore solution of salt-saturated concrete and can usually be taken as the concentration of immersed salt solution, which is 4.0×10^6 mol/m^3; and f is the correction factor, which is 1.0.

2.3.3. Water Permeability Test

The water permeability test was conducted according to the Chinese Standard JTG E30-2005 [53]. A concrete sample (frustum of a cone) with a top surface diameter of 175 mm, a bottom diameter of 185 mm, and a height of 150 mm was used for the test. At 28 days, the side of the sample was coated with epoxy resin and dried before the tests. The top surface of the sample was subjected to a constant water pressure of 0.8 MPa ± 0.05 MPa for 24 h, and then the sample was taken out and split into 2 halves to trace the water ingress depth. The average water ingress depth of 10 measured positions along the split surface of the sample. The water permeability coefficient was then calculated by Equation (2):

$$S_k = \frac{mD_m^2}{2TH} \tag{2}$$

where S_k is the water permeability coefficient, mm/s; D_m is the average water seepage height, cm; H is the water pressure, expressed in height of water column, cm; T is the test time under the constant water pressure, hours; and m is the the water absorption of concrete and is generally taken as 0.03.

2.3.4. Pore Size Distribution Test

The pore size distribution of the concrete sample was measured through an automated mercury porosimeter Micromeritics AutoPore Iv 9510. Selected broken mortar samples were used for the tests. The samples were firstly immersed in absolute ethyl alcohol for 72 h, followed by oven-drying under 40 °C for 24 h to remove any moisture inside, and then stored under vacuum condition before the tests.

3. Results

3.1. Effect of AMF Content on Performance of Machine-Made Sand Concrete

3.1.1. Effect of AMF Content on the Slump of Machine-Made Sand Concrete

The effect of AMF content on the properties of the concrete was studied when the AMF content was 0%, 5%, 10%, 15% and 20% in machine-made sand. The slump of fresh concrete increased firstly and then decreased with the increase of AMF content, as shown in Figure 2. The AMF could be filled in the pores of the fresh concrete, and at the same time, the water in the original pores was released and became free water, as evidenced by the improvement of workability and a higher slump of the concrete. However, excessive AMF could sharply increase the total specific surface area of the powders, resulting in a higher water demand and a lower slump.

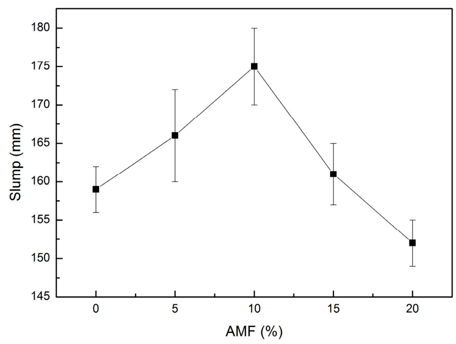

Figure 2. Effect of AMF content on slump of fresh concrete.

3.1.2. Effect of AMF Content on the Compressive Strength of Machine-Made Sand Concrete

The compressive strength of the concretes with different AMF contents is shown in Figure 3. Although there was no significant difference between the compressive strength of the concretes at 7 days, the results at 28 days showed a similar pattern as in Figure 2. When the content of AMF was 10%, the compressive strength of concrete at 28 days was the highest, which was 12.1% higher than that without AMF. When the AMF filled the pores, it also increased the tightness and compactness of the concrete. The hardened concrete had a higher packing density and a higher strength. Excessive AMF resulted into a poor workability, poor compactness, and thus a decrease in strength.

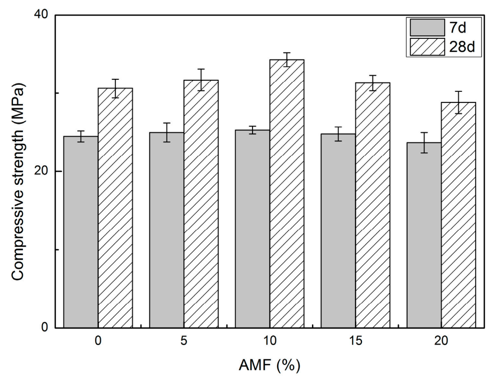

Figure 3. Effect of AMF content on the compressive strength of concrete.

3.1.3. Effect of AMF Content on the Permeability of Machine-Made Sand Concrete

The effect of AMF content on the water permeability coefficient and chloride permeability coefficient is shown in Figure 4. It can be seen from the figure that the influence of AMF on the permeation resistance of concrete was consistent with the effect on compressive strength. When the content of AMF was 10%, the water permeability coefficient and chloride permeability coefficient reached the lowest values.

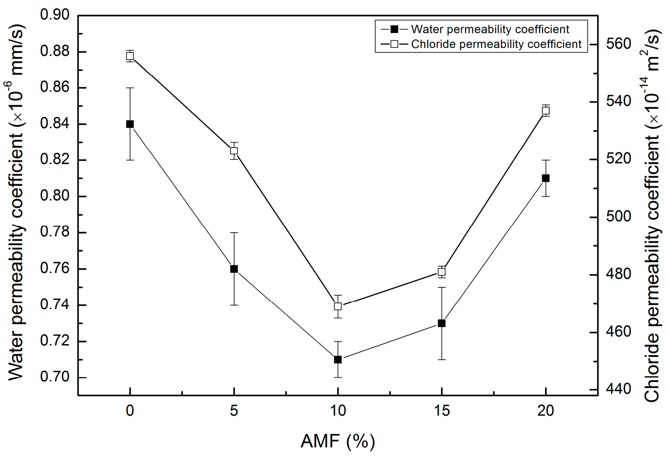

Figure 4. Effect of AMF content on the permeability of concrete.

In summary, the overall performance of the concrete was the best when the AMF content was 10%. This is because the optimum content of the AMF particles (<75 μm) could fill the gap/pores between the cement particles, making the accumulation between the particles more compact [54,55]. Therefore, the compressive strength of concrete was improved, and the permeability resistance of concrete was improved accordingly.

3.2. *Effect of Aluminum Sulfate on Performance of Machine-Made Sand Concrete*

In order to further improve the performance of the machine-made sand concrete, based on the optimum content of 10% AMF, the aluminum sulfate was added, and the influence of aluminum sulfate on the slump, compressive strength, and water/chloride permeability was investigated.

3.2.1. Effect of Aluminum Sulfate Content on the Slump of Machine-Made Sand Concrete

The effect of 0%, 0.5%, 1%, and 2% of aluminum sulfate by weight of the cementitious materials on the properties of the concrete was studied. Figure 5 shows that the slump of fresh concrete decreased when the amount of aluminum sulfate was increased. This is because, when the $Ca(OH)_2$ was formed through the hydration reaction of the main minerals C_3S and C_2S in the OPC as shown in Equation (3), the existence of aluminum sulfate contributed to the formation of ettringite through the reaction with $Ca(OH)_2$, as shown in Equation (4) [44]. The existence of more ettringite decreased the workability and slump of concrete.

$$3CaO{\cdot}SiO_2{+}nH_2O \ \rightarrow xCaO{\cdot}SiO_2{\cdot}yH_2O + (3-x)Ca(OH)_2 \tag{3}$$

$$Al_2(SO)_4{\cdot}18H_2O + 6Ca(OH)_2 \overset{H_2O}{\rightarrow} 3CaO{\cdot}Al_2O_3{\cdot}3CaSO_4{\cdot}32H_2O \tag{4}$$

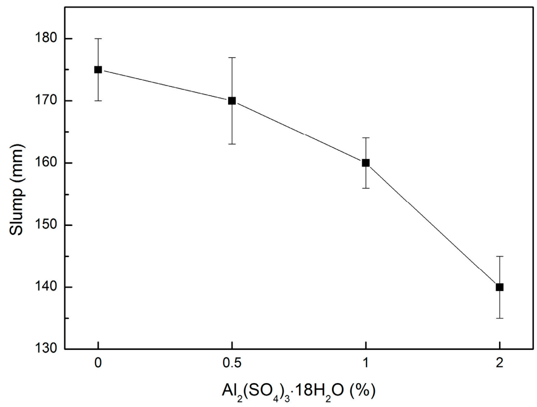

Figure 5. Effect of aluminum sulfate on slump of fresh concrete.

3.2.2. Effect of Aluminum Sulfate Content on the Compressive Strength of Machine-Made Sand Concrete

It can be seen from Figure 6 that, when the amount of aluminum sulfate was increased from 0% to 2%, the compressive strength of the concrete firstly increased and then decreased. When the aluminum sulfate content was 1%, the compressive strength of concrete at 7 and 28 days was the highest, respectively at 32.8 MPa and 37.9 MPa, which were increased by 29.6% and 10.5% compared to the mix with 0% of aluminum sulfate. This shows that aluminum sulfate is advantageous for concrete strength when the optimum content is added. However, excess amounts of aluminum sulfate could cause an increase in pore size and microcracks inside the concrete [56], and thus decrease the compressive strength.

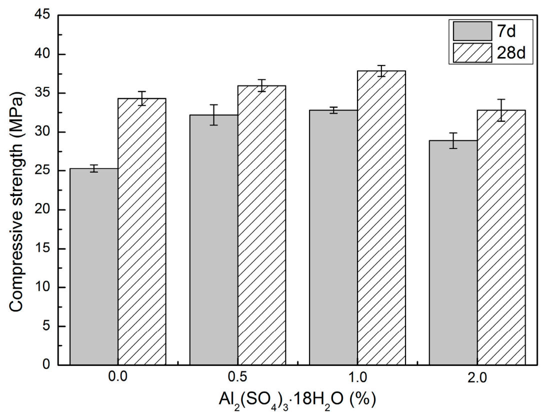

Figure 6. Effect of aluminum sulfate on the compressive strength of concrete.

3.2.3. Effect of Aluminum Sulfate Content on the Permeability of Machine-Made Sand Concrete

Figure 7 shows that, when the amount of aluminum sulfate was increased, the concrete water permeability and chloride permeability coefficients firstly decreased and then increased. When the content was 1%, the two permeability coefficients of the concrete reached the minimum values. When the content was 1%, the water and chloride permeability coefficients were reduced by 22.5% and 19.5% compared to those of the sample with no aluminum sulfate. This shows that the aluminum sulfate could improve the impermeability of the concrete when the content was within the optimum content. This is because the aluminate sulfate accelerated and increased the formation of ettringite, which filled the pores and compensated for any microcracks caused by volume shrinkage during cement hydration, thereby improving the rigidity and waterproof ability of the concrete. Too much aluminum sulfate could increase the pore size and the microcracks as reported in literature [56], and increase the permeability of the concrete.

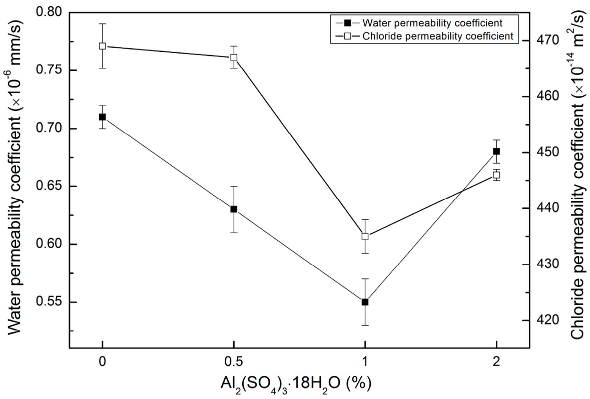

Figure 7. Effect of aluminum sulfate on the permeability of concrete.

In summary, when the aluminum sulfate content was less than 1%, the impermeability of concrete was improved. In addition, the concrete had the best impermeability when the content was 1%. At the same time, aluminum sulfate also promoted the early strength of concrete; however, the slump of fresh concrete was slightly decreased. It was the ettringite formed by the reaction of aluminum sulfate with $Ca(OH)_2$ which decreased the pores in the concrete, thereby improving the impermeability of the concrete. On the other hand, aluminum sulfate simultaneously introduced some free Al^{3+} ions, which could restrain the movement of Cl^- in the pores of the concrete.

3.3. Effect of PPF on Performance of Machine-Made Sand Concrete

3.3.1. Effect of PPF Content on the Slump of Machine-Made Sand Concrete

PPF of 0.6 kg/m^3, 0.9 kg/m^3 and 1.35 kg/m^3 were blended into the concrete to study the effect of PPF on the properties of concrete. As shown in Figure 8, the slump of fresh concrete decreased continuously with an increase in PPF. The result suggests that excessive PPF was unfavorable for the workability of the fresh concrete.

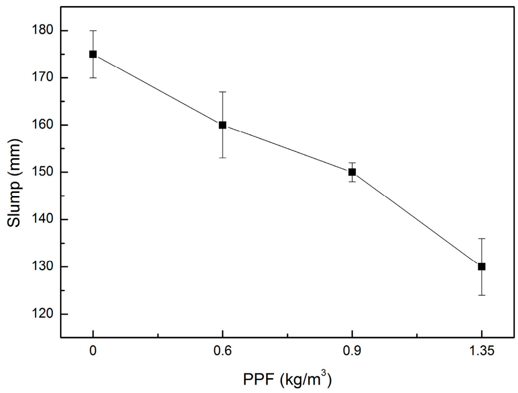

Figure 8. Effect of PPF on the slump of fresh concrete.

3.3.2. Effect of PPF Content on the Compressive Strength of Machine-Made Sand Concrete

It can be seen from Figure 9 that with the increase in PPF content, the compressive strength of the concrete showed a significant increase and then a decreasing trend. When the PPF was 0.6 kg/m^3, the compressive strength of concrete at 7 and 28 days reached the maximum values of 31.5 MPa and 41.6 MPa, respectively, which were 24.5% and 21.3% higher than those of the concrete with no PPF. The optimum content of PPF could increase the crack resistance of concrete by providing a good bonding property between the PPF and the cement matrix, but too much PPF could decrease the bonding property because there was insufficient cement matrix to accommodate the excess PPF, thereby decreasing the compressive strength.

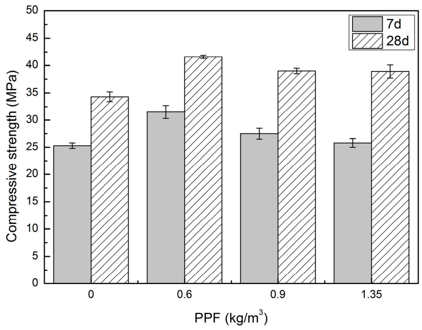

Figure 9. Effect of PPF on compressive strength of concrete.

3.3.3. Effect of PPF Content on the Permeability of Machine-Made Sand Concrete

The effect of PPF content on the water and chloride permeability coefficients of the concrete is shown in Figure 10. It can be seen that with an increase in the PPF content, both the water permeability coefficient and chloride permeability coefficient decreased first and then increased. When the PPF content was 0.6 kg/m^3, the permeability coefficients were the lowest, and the decrease in water and chloride permeability coefficients was 46.5% and 51.1%, respectively, compared to that of the concrete with no PPF. Even when the PPF content was 0.9 kg/m^3, the two permeability coefficients were still lower than those of the concrete with no PPF. When the PPF content was 1.35 kg/m^3, the water permeability coefficient was higher than the that of the concrete with no PPF. This indicates that the PPF has an advantage on improving the impermeability of the concrete when the PPF content is ≤0.9 kg/m^3. This is due to the fact that on the one hand, in the alkaline environment of concrete, the adhesion between the PPF and the cement matrix was enhanced [27]. On the other hand, the PPF restricted the formation of microcracks caused by any shrinkage of the concrete, thereby reducing the transportation channels for water and chloride ions. In addition, a large number of evenly distributed PPF in the concrete could block the capillary pores inside the concrete [17].

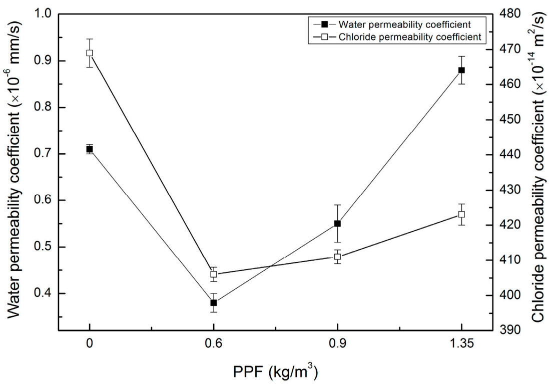

Figure 10. Effect of PPF on permeability of concrete.

3.4. Pore Size Analysis

Figure 11 shows the pore size distribution of the concrete samples with different contents of AMF, aluminum sulfate, and PPF. It can be seen that the incorporation of AMF, aluminum sulfate, and PPF significantly reduced the pore size and the overall porosity of the concrete. In Figure 11a, the pore size distribution of the concrete with 0% and 10% AMF is compared. The AMF exhibited a filling effect, and the porosity of the concrete was remarkably decreased in the concrete with 10% AMF. The pores in the concrete with 10% AMF were mainly distributed in the range of 10–100 nm, compared with the case that the pores in the concrete with no AMF were mainly distributed in the range of 10–2000 nm.

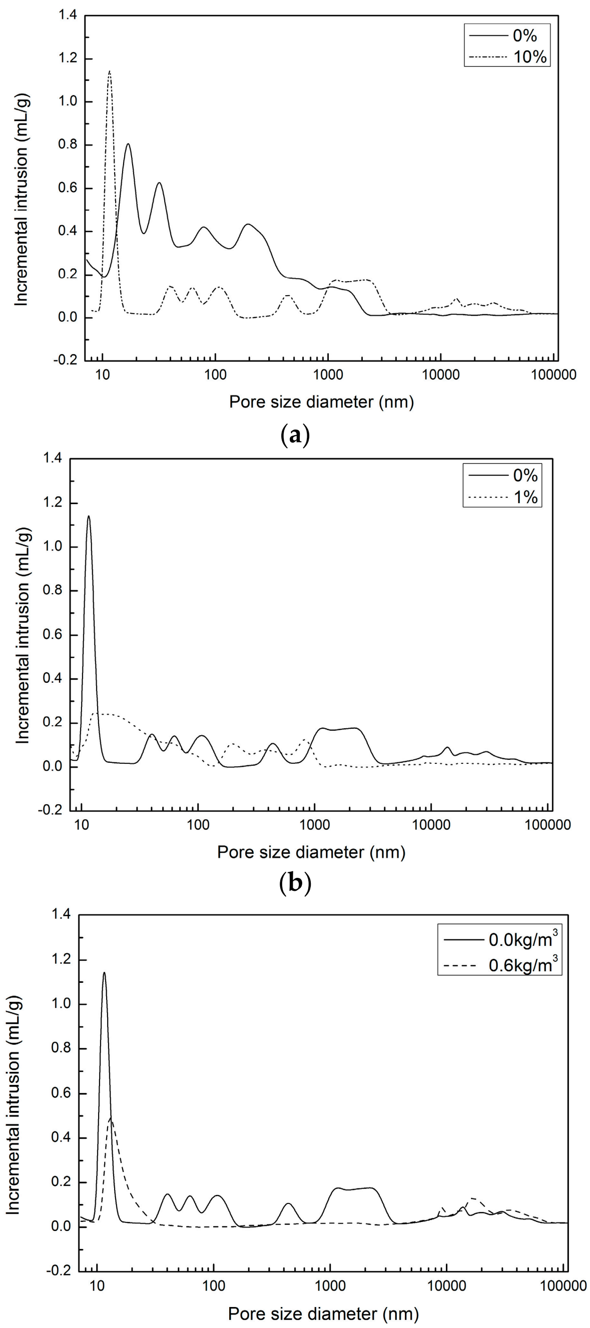

(c)

Figure 11. Pore size distribution results of concrete with different contents of: (**a**) AMF; (**b**) aluminum sulfate; (**c**) PPF.

Under the condition that the optimum content of AMF (10%) was added, the effect of aluminum sulfate and PPF on the pore size distribution are shown in Figure 11b,c. In Figure 11b, when the aluminum sulfate content was 1%, the pore size distribution was more uniform than that of the concrete with no aluminum sulfate. The amount of small pores in the range of 20–1000 nm increased, and the amount of large pores >1000 nm was significantly reduced. It is known that the large pores should be controlled to a minimum level in order to achieve a low permeability property. In Figure 11c, the PPF clearly reduced the total porosity of the concrete, and the pores of the concrete were focused between 10–30 nm. This optimized the pore distribution in concrete and the concrete microstructure was more compact, reflected by the improvement of the resistance of permeability.

4. Discussion

With the demand of using machine-made sand in concrete, the possible methods to improve the properties of MSC should be investigated. In this study, the effects of adding AMF, aluminum sulfate and PPF on the slump, compressive strength, and water and chloride permeability coefficients of MSC were investigated. The findings should provide a guidance for the mix design of MSC in related construction projects. Future research could be carried out include a multiple factor analysis on the combined use of all the three additions (AMF, aluminum sulfate, and PPF), and other types of minerals such as ground granulated blast-furnace, fly ash, and silica fume, on the related properties of MSC.

5. Conclusions

The effects of AMF content, aluminum sulfate, and PPF on MSC performance, including the slump, compressive strength and permeability, were studied. The main conclusions were as follows:

(1) With an increase of AMF content, the compressive strength of MSC first increased and then decreased. The permeability coefficients of water and chloride first decreased and then increased. They all achieved the best performance when the content of AMF was 10wt% in the machine-made sand. AMF was found to be able to effectively reduce the pores in the range of 20–1000 nm in the MSC.

(2) With an increase in the content of aluminum sulfate, the permeability coefficients of water and chloride decreased first and then increased. When the content of aluminum sulfate was 1%, the two permeability coefficients reached the minimum value. At the same time, MSC had the highest compressive strength. The aluminate sulfate was found to be able to decrease the pores in the range >1000 nm in the MSC.

(3) The water and chloride permeability coefficients firstly decreased and then increased with an increase in PPF content. When the PPF content was 0.6 kg/m^3, the MSC reached the optimum performance with only a slight decrease in the slump of fresh concrete, the highest compressive strength (increase by more than 20% compared with no PPF), and the lowest water and chloride permeability coefficients (decrease by more than 45% compared with no PPF).

(4) The optimum content of AMF contributed to a good filling effect and modify the pore structure of MSC, thereby increasing the compressive strength and impermeability of MSC. Aluminum sulfate could promote the formation of ettringite. The filling effect of ettringite in the pores made the MSC structure denser, and the porosity of MSC was reduced. PPF (0.6 kg/m^3) was found to effectively decrease the pores with a size 30–3000 nm in MSC, and thus increase the impermeability.

Author Contributions: Conceptualization, J.W. and Y.W.; methodology, J.W. and Y.W.; formal analysis, J.W. and Y.W.; investigation, H.H.; data curation, H.H.; writing—original draft preparation, H.H. and J.W.; writing—review and editing, J.W. and H.H.; supervision, J.W.; project administration, J.W. and Y.W.; funding acquisition, Y.W.

Funding: This research was funded by National Natural Science Foundation of China (51678220), the Program for Innovation Scientists and Technicians Troop Construction Projects of Henan Province in China (CXTD2017088) and the Program for Innovative Research Team (in Science and Technology) (19IRTSTHN027) in Henan Polytechnic University are appreciated.

Acknowledgments: The authors appreciate the support from the Engineering division in New York University Abu Dhabi, UAE.

Conflicts of Interest: The authors declare no conflict of interest.

References

1. Rajput, S.P.S. An Experimental study on Crushed Stone Dust as Fine Aggregate in Cement Concrete. *Mater. Today-Proc.* **2018**, *5*, 17540–17547. [CrossRef]
2. Meisuh, B.K.; Kankam, C.K.; Buabin, T.K. Effect of quarry rock dust on the flexural strength of concrete. *Case Stud. Constr. Mater.* **2018**, *8*, 16–22. [CrossRef]

3. Kankam, C.K.; Meisuh, B.K.; Sossou, G.; Buabin, T.K. Stress-strain characteristics of concrete containing quarry rock dust as partial replacement of sand. *Case Stud. Constr. Mater.* **2017**, *7*, 66–72. [CrossRef]
4. Cepuritis, R.; Jacobsen, S.; Pedersen, B.; Mortsell, E. Crushed sand in concrete—Effect of particle shape in different fractions and filler properties on rheology. *Cem. Concr. Compos.* **2016**, *71*, 26–41. [CrossRef]
5. Cepuritis, R.; Wigum, B.J.; Garboczi, E.J.; Mortsell, E.; Jacobsen, S. Filler from crushed aggregate for concrete: Pore structure, specific surface, particle shape and size distribution. *Cem. Concr. Compos.* **2014**, *54*, 2–16. [CrossRef]
6. Cepuritis, R.; Garboczi, E.J.; Ferraris, C.F.; Jacobsen, S.; Sorensen, B.E. Measurement of particle size distribution and specific surface area for crushed concrete aggregate fines. *Adv. Powder Technol.* **2017**, *28*, 706–720. [CrossRef]
7. Galetakis, M.; Soultana, A. A review on the utilisation of quarry and ornamental stone industry fine by-products in the construction sector. *Constr. Build. Mater.* **2016**, *102*, 769–781. [CrossRef]
8. Abou-Zeid, M.; Fakhry, M. Short-term impact of high-aggregate fines content on concrete incorporating water-reducing admixtures. *Aci Mater. J.* **2003**, *100*, 280–285.
9. Ahmed, A.; Elkourd, A. Properties of Concrete Incorporating Natural and Crushed Stone very Fine Sand. *ACI Mater. J.* **1989**, *86*, 417–424.
10. Celik, T.; Marar, K. Effects of crushed stone dust on some properties of concrete. *Cem. Concr. Res.* **1996**, *26*, 1121–1130. [CrossRef]
11. Shen, W.; Liu, Y.; Wang, Z.; Cao, L.; Wu, D.; Wang, Y.; Ji, X. Influence of manufactured sand's characteristics on its concrete performance. *Constr. Build. Mater.* **2018**, *172*, 574–583. [CrossRef]
12. Nanthagopalan, P.; Santhanam, M. Fresh and hardened properties of self-compacting concrete produced with manufactured sand. *Cem. Concr. Compos.* **2011**, *33*, 353–358. [CrossRef]
13. Svermova, L.; Sonebi, M.; Bartos, P. Influence of mix proportions on rheology of cement grouts containing limestone powder. *Cem. Concr. Compos.* **2003**, *25*, 737–749. [CrossRef]
14. Wang, Y.; He, H.; Liu, X. Influences of aggregate micro fines on the packing of fresh mortar and the performances of mortar. *Compos. Part B-Eng.* **2019**, *164*, 493–498.
15. Farzampour, A. Compressive Behavior of Concrete under Environmental Effects. In *Compressive Strength of Concrete*; Pavlo, K., Ed.; IntechOpen: London, UK, 2019; pp. 1–12.
16. Cepuritis, R.; Jacobsen, S.; Smeplass, S.; Mortsell, E.; Wigum, B.J.; Ng, S. Influence of crushed aggregate fines with micro-proportioned particle size distributions on rheology of cement paste. *Cem. Concr. Compos.* **2017**, *80*, 64–79. [CrossRef]
17. Matar, P.; Assaad, J.J. Concurrent effects of recycled aggregates and polypropylene fibers on workability and key strength properties of self-consolidating concrete. *Constr. Build. Mater.* **2019**, *199*, 492–500. [CrossRef]
18. Zhang, P.; Li, Q. Effect of polypropylene fiber on fracture properties of high-performance concrete composites. *Sci. Eng. Compos. Mater.* **2012**, *19*, 407–414. [CrossRef]
19. Aslani, F.; Gedeon, R. Experimental investigation into the properties of self-compacting rubberised concrete incorporating polypropylene and steel fibers. *Struct. Concr.* **2019**, *20*, 267–281. [CrossRef]
20. Xu, L.; Li, B.; Ding, X.; Chi, Y.; Li, C.; Huang, B.; Shi, Y. Experimental Investigation on Damage Behavior of Polypropylene Fiber Reinforced Concrete under Compression. *Int. J. Concr. Struct. Mater.* **2018**, *12*, 68. [CrossRef]
21. Niu, D.; Huang, D.; Zheng, H.; Su, L.; Fu, Q.; Luo, D. Experimental Study on Mechanical Properties and Fractal Dimension of Pore Structure of Basalt Polypropylene Fiber-Reinforced Concrete. *Appl. Sci.* **2019**, *9*, 1602. [CrossRef]
22. Pakravan, H.R.; Latifi, M.; Jamshidi, M. Hybrid short fiber reinforcement system in concrete: A review. *Constr. Build. Mater.* **2017**, *142*, 280–294. [CrossRef]
23. Wang, D.; Ju, Y.; Shen, H.; Xu, L. Mechanical properties of high performance concrete reinforced with basalt fiber and polypropylene fiber. *Constr. Build. Mater.* **2019**, *197*, 464–473. [CrossRef]
24. Alhozaimy, A.; Soroushian, P.; Mirza, F. Mechanical properties of polypropylene fiber reinforced concrete and the effects of pozzolanic materials. *Cem. Concr. Compos.* **1996**, *18*, 85–92. [CrossRef]
25. De Alencar Monteiro, V.M.; Lima, L.R.; Silva, F.d.A. On the mechanical behavior of polypropylene, steel and hybrid fiber reinforced self-consolidating concrete. *Constr. Build. Mater.* **2018**, *188*, 280–291. [CrossRef]
26. Akca, K.R.; Cakir, O.; Ipek, M. Properties of polypropylene fiber reinforced concrete using recycled aggregates. *Constr. Build. Mater.* **2015**, *98*, 620–630. [CrossRef]

27. Rostami, R.; Zarrebini, M.; Mandegari, M.; Sanginabadi, K.; Mostofinejad, D.; Abtahi, S.M. The effect of concrete alkalinity on behavior of reinforcing polyester and polypropylene fibers with similar properties. *Cem. Concr. Compos.* **2019**, *97*, 118–124. [CrossRef]
28. Gupta, S.; Kua, H.W.; Cynthia, S.Y.T. Use of biochar-coated polypropylene fibers for carbon sequestration and physical improvement of mortar. *Cem. Concr. Compos.* **2017**, *83*, 171–187. [CrossRef]
29. Qin, Y.; Zhang, X.; Chai, J.; Xu, Z.; Li, S. Experimental study of compressive behavior of polypropylene-fiber-reinforced and polypropylene-fiber-fabric-reinforced concrete. *Constr. Build. Mater.* **2019**, *194*, 216–225. [CrossRef]
30. Yew, M.K.; Bin Mahmud, H.; Ang, B.C.; Yew, M.C. Influence of different types of polypropylene fibre on the mechanical properties of high-strength oil palm shell lightweight concrete. *Constr. Build. Mater.* **2015**, *90*, 36–43. [CrossRef]
31. Afroughsabet, V.; Ozbakkaloglu, T. Mechanical and durability properties of high-strength concrete containing steel and polypropylene fibers. *Constr. Build. Mater.* **2015**, *94*, 73–82. [CrossRef]
32. Sun, Z.; Xu, Q. Microscopic, physical and mechanical analysis of polypropylene fiber reinforced concrete. *Mater. Sci. Eng. A-Struct. Mater. Prop. Microstruct. Process.* **2009**, *527*, 198–204. [CrossRef]
33. Das, C.S.; Dey, T.; Dandapat, R.; Mukharjee, B.B.; Kumar, J. Performance evaluation of polypropylene fibre reinforced recycled aggregate concrete. *Constr. Build. Mater.* **2018**, *189*, 649–659. [CrossRef]
34. Hiremath, P.N.; Yaragal, S.C. Performance evaluation of reactive powder concrete with polypropylene fibers at elevated temperatures. *Constr. Build. Mater.* **2018**, *169*, 499–512. [CrossRef]
35. Nili, M.; Afroughsabet, V. The effects of silica fume and polypropylene fibers on the impact resistance and mechanical properties of concrete. *Constr. Build. Mater.* **2010**, *24*, 927–933. [CrossRef]
36. Zhang, P.; Li, Q. Effect of polypropylene fiber on durability of concrete composite containing fly ash and silica fume. *Compos. Part B-Eng.* **2013**, *45*, 1587–1594. [CrossRef]
37. Li, Y.; Zhang, Y.; Yang, E.; Tan, K.H. Effects of geometry and fraction of polypropylene fibers on permeability of ultra-high performance concrete after heat exposure. *Cem. Concr. Res.* **2019**, *116*, 168–178. [CrossRef]
38. Sadiqul Islam, G.M.; Gupta, S.D. Evaluating plastic shrinkage and permeability of polypropylene fiber reinforced concrete. *Int. J. Sustain. Built Environ.* **2016**, *5*, 345–354. [CrossRef]
39. Karahan, O.; Atis, C.D. The durability properties of polypropylene fiber reinforced fly ash concrete. *Mater. Des.* **2011**, *32*, 1044–1049. [CrossRef]
40. Afroughsabet, V.; Biolzi, L.; Monteiro, P.J.M. The effect of steel and polypropylene fibers on the chloride diffusivity and drying shrinkage of high-strength concrete. *Compos. Part B-Eng.* **2018**, *139*, 84–96. [CrossRef]
41. Chen, Y.; Cen, G.; Cui, Y. Comparative study on the effect of synthetic fiber on the preparation and durability of airport pavement concrete. *Constr. Build. Mater.* **2018**, *184*, 34–44. [CrossRef]
42. Cao, L.; Shi, X.; Liu, X.; Wu, J. Laboratory study on the properties of plastering mortar modified by feather fibers. *Sci. Eng. Compos. Mater.* **2013**, *20*, 293–299. [CrossRef]
43. Olivier, G.; Combrinck, R.; Kayondo, M.; Boshoff, W.P. Combined effect of nano-silica, super absorbent polymers, and synthetic fibres on plastic shrinkage cracking in concrete. *Constr. Build. Mater.* **2018**, *192*, 85–98. [CrossRef]
44. Wang, Y.; He, H.; He, F. Effect of slaked lime and aluminum sulfate on the properties of dry-mixed masonry mortar. *Constr. Build. Mater.* **2018**, *180*, 117–123. [CrossRef]
45. Wang, Y.; Yu, J.; Wang, J.; Guan, X. Effects of Aluminum Sulfate and Quicklime/Fluorgypsum Ratio on the Properties of Calcium Sulfoaluminate (CSA) Cement-Based Double Liquid Grouting Materials. *Materials* **2019**, *12*, 1222. [CrossRef]
46. Chen, C.; Sun, Z. Influence of Aluminum Sulfate on Hydration and Properties of Cement Pastes. *J. Adv. Concr. Technol.* **2018**, *16*, 522–530. [CrossRef]
47. *Standardization Administration of the People's Republic of China, GB175-2007: Common Portland Cement*; China Architecture and Building Press: Beijing, China, 2007.
48. *National Standard of the People's Republic of China, GB/T 14685-2011 Pebble and Crushed Stone for Construction*; Chinese National Standard: Beijing, China, 2011.
49. *National Standards of the People's Republic of China, GB/T 14684-2011 Sand for Construction*; Standardization Administration of China: Beijing, China, 2011.
50. *Standardization Administration of the People's Republic of China, GB/T 50080-2016: Standard for Test Method of Performance on Ordinary Fresh Concrete*; China Architecture & Building Press: Beijing, China, 2016.

51. Wang, X.; Lee, H. Modeling of chloride diffusion in concrete containing low-calcium fly ash. *Mater. Chem. Phys.* **2013**, *138*, 917–928. [CrossRef]
52. Lu, X. Application of the Nernst-Einstein equation to concrete. *Cem. Concr. Res.* **1997**, *27*, 293–302. [CrossRef]
53. *Profession Standard of The People's Republic of China, JTG E30-2005 Test Method of Cement and Concrete for Highway Engineering*; Ministry of Communications of the People's Republic of China: Beijing, China, 2005.
54. Wang, Y.; Jin, Z.; Liu, S.; Yang, L.; Luo, S. Physical filling effect of aggregate micro fines in cement concrete. *Constr. Build. Mater.* **2013**, *41*, 812–814. [CrossRef]
55. Rizwan, S.A.; Bier, T.A. Blends of limestone powder and fly-ash enhance the response of self-compacting mortars. *Constr. Build. Mater.* **2012**, *27*, 398–403. [CrossRef]
56. Tian, K.; Chen, K.; Zhuang, L.; Shang, X.; Li, C.; Gao, R. Influence of alkali-free liquid quick-setting agent on the hydration and properties of Portland cement at low temperature. *New Build. Mater.* **2018**, *12*, 72–85.